FAILURE AND PENETRATION RESPONSE OF BOROSILICATE GLASS DURING SHORT ROD IMPACT

Th. Behner[1], C. E. Anderson Jr[2]., D. L. Orphal[3], M. Wickert[1], V. Hohler[1] and D. W. Templeton[4]

[1] *Fraunhofer Institut für Kurzzeitdynamik (EMI), Eckerstr. 4, 79104 Freiburg, Germany*
[2] *Southwest Research Institute, P.O. Drawer 28510, San Antonio, TX 78228, USA*
[3] *International Research Associates, Inc., 4450 Black Avenue, Pleasanton, CA 94566, USA*
[4] *U. S. Army TARDEC-RDECOM, AMSRD-TAR-R, Warren, MI 48397, USA*

A test series with short gold rods as the projectile and borosilicate glass as the target was carried out to investigate whether the failure front in the glass remains "steady" after the driving stress from the penetrating rod is removed. Impact velocities from ≈ 1 km/s to 2 km/s were investigated. Results show that the failure front induced by the rod impact can cease propagating after the rod is totally eroded inside the glass. Interestingly, cessation of the propagating front is delayed in time from the point when the rod is completely eroded.

INTRODUCTION

Failure characterization of brittle materials like ceramics or glass is of fundamental importance in describing the resistance of these types of materials against impact of projectiles. The failure phenomenon for glasses during dynamic loading is usually investigated by applying a planar impact test, Taylor test, or long-rod impact [1-7]. A failure wave or failure front, which propagates from the impact zone into the undamaged part of the glass, can easily be observed. A critical question is whether this failure front remains "steady" after the driving stress from either the planar plate or the penetrating rod is removed. That is, does failure propagate similar to a wave propagating without a driving force, or is it failure-kinetics based with a slow down or come to a standstill after the stress is removed?

Results of a test series with short gold rods impacting borosilicate glass investigating this fundamental question are reported in this paper. Impact velocities between 1 and 2 km/s were considered. Very high-accuracy measurements were established to ensure reliable results. Failure and penetration response of the glass were monitored simultaneously with flash X-rays and high-speed photography. These allow observation of the failed region of the glass (photography), and the position and length of the rod (X-rays) inside the failed region.

EXPERIMENTAL SET-UP

The borosilicate glass targets were cylindrical with diameter D = 21 mm and a length of L = 60 mm. The material properties are given in Table 1. The rods were made of pure gold (99.99%) and had a diameter of d = 1 mm and varying lengths of $l_{rod} \approx 5$ to 11 mm with the following material properties: density ρ_P = 19.3 g/cm³; hardness 65 HV5; UTS 220 MPa; and elongation 30%. For the experiments the reverse ballistic method was used and the impact and penetration process was observed simultaneously with five 180-kV flash X-rays, and an IMACON 200 high-speed optical camera that took 16 pictures to visualize failure propagation in the glass. The test set-up was similar to that described in [5]; only the rod was mounted differently and the angles of the X-ray tubes with respect to the target plane were changed. Figure 1 shows the arrangement for the impact tank together with a resulting X-ray image of the penetration process. The tests were performed with a two-stage light-gas gun using a separating sabot to launch the glass targets. The rod was suspended by attaching it to a stripe of cello tape and then aligned in the trajectory with the aid of a laser.

The time measurements for the flash X-ray pictures are very accurate (to better than ±5 ns). Thus, the error for the velocities determined from the X-ray pictures rest in the accuracy of the position measurement, which is in the order of ± 0.1 to 0.15 mm. The camera pictures allowed a position accuracy in the order of < ± 0.2 mm, caused mainly by irregularities in the shape of the failure front.

Table 1: Material properties for borosilicate glass (Borofloat® 33)

Density [g/cm³]	Young's modulus [GPa]	Knoop hardness [kp/mm²]	Poisson's ratio	longitudinal wavespeed [km/s]	transverse wavespeed [km/s]	HEL [4] [GPa]
2.2	64	480	0.2	5.69	3.48	8

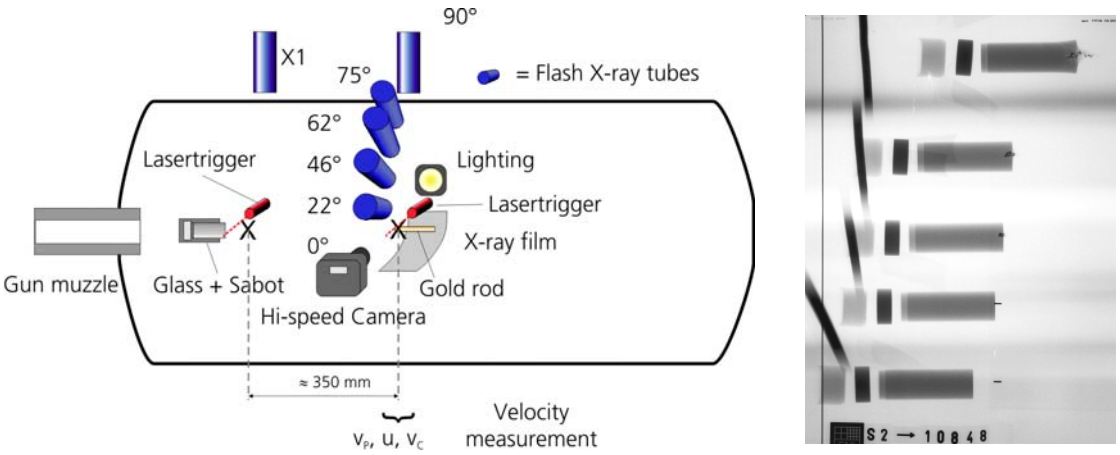

Figure 1. Test-set-up – reverse ballistic method – and resulting X-ray photograph

RESULTS AND DISCUSSION

Experimental results are listed in Table 2. Impact velocity v_P, penetration velocity u and consumption velocity v_C of the rod were calculated by a linear regression of the position and length of the rod versus the trigger time of each X-ray image. The camera pictures provided the failure front velocity v_F inside the glass. Target resistance R_T was calculated from the well known Tate equation using the u and v_C values and with a penetrator strength $Y_P = 0$.

To evaluate the failure and penetration response of the glass it is helpful to estimate the time and position when the rod is totally eroded inside the glass. These values can be calculated from u, v_C and l_{rod} if the effects of deceleration at the end of the penetration process are not considered.

Camera pictures of the failure front and X-ray images of the penetration process after impact are shown in Figs. 2 and 3 for different v_P and l_{rod}. For Exp. 10848 (Fig.2, $v_P \approx 950$ m/s) the calculated point of total rod erosion is at 12.2 µs after impact with a penetration depth of 6.5 mm (same time as the 3rd X-ray image). A few µs after the rod is eroded, the failure front inside the glass comes to a standstill (camera pictures 2-4). From the backside of the glass cylinder, another failure front develops, which could be the result of (multiple) reflections of the shock front at the rear. However, it can be clearly seen that the original failure front does not move from a time of 18 µs to 83 µs.

This is illustrated in Fig. 4 which shows the evaluated data of Exp 10848 as a position-time graph. While the failure front propagates in the glass, the behavior is very linear; the slope of the regression line denotes v_F. A few µs after the rod is completely eroded, failure front propagation stops and its position stays constant for the remainder of the observation time.

Table 2. Experimental results

Exp. No. -	Yaw [°]	oc [mm]	v_P [m/s]	u [m/s]	v_C [m/s]	v_F [m/s]	R_T [GPa]	l_{rod} [mm]
10848	1.7	1.8	948±13	528±37	437±18	1454±53	1.53	5.3
10845	1.7	2.0	971±6	446	490	1564±65	2.10	6.6
10841	1.6	3.8	1462±17	863±34	620±15	1952±30	2.89	11.1
10842	3.5	1.5	1489±21	890±38	579±50	2028±35	2.37	6.8
10843	2.0	2.7	1989±6	1254±19	727±3	2048±76	3.37	10.0
10864	2.7	2.6	2015±22	1332±39	680±1	2232±44	2.51	11.4
10846	1.3	1.8	2043	1354	690	2041±31	2.58	9.7
10849	2.3	2.9	2066±9	1330	719	2222±145	3.04	6.8

Yaw: combined horizontal and vertical yaw
oc: off-centre impact

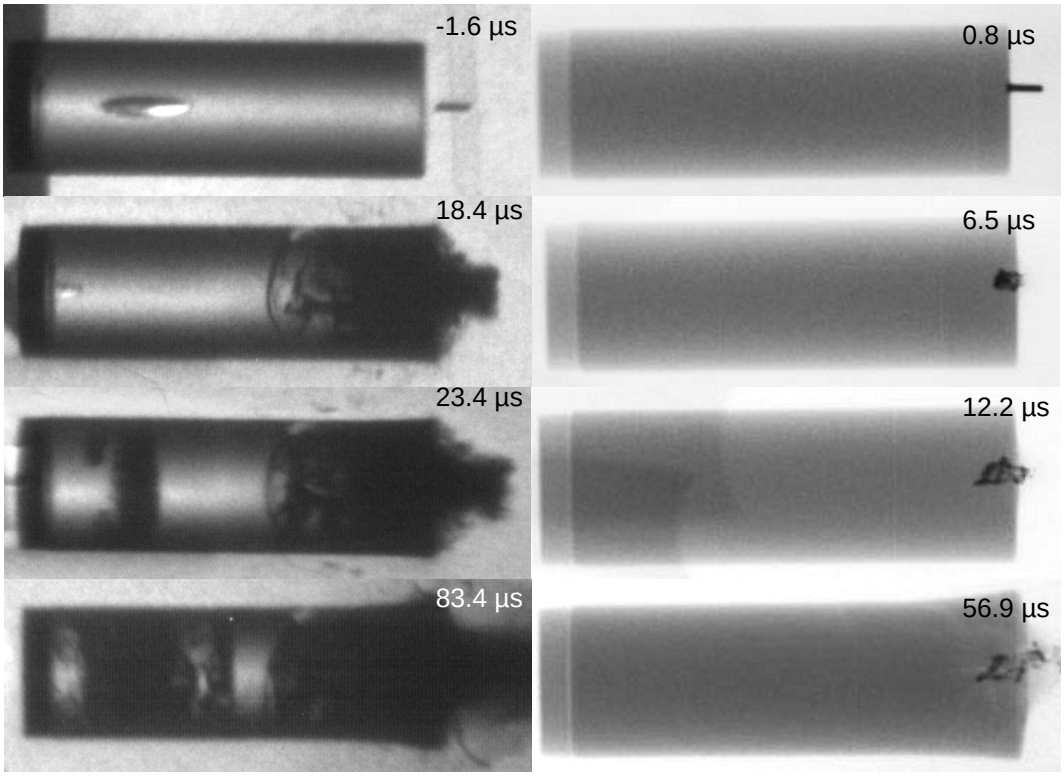

Figure 2. Camera pictures (left) and X-ray images (right) for Exp. 10848 (v_P = 948 m/s); times after impact

At higher impact velocities (Figs. 3 and 5, Exp. 10864, $v_P \approx 2$ km/s) the limited length of the glass target prevents a complete observation of cessation of failure front propagation. However, with the point of total rod erosion for Exp 10864 calculated at 16.7 µs and 22.3-mm penetration depth (shortly after X-ray image 3), camera pictures 3 and 4 show at least a slowdown of the failure front, which can be interpreted as the beginning of cessation of the propagating front. Experiments with longer glass rods are planned to validate this behavior.

Figures 4 and 5 show that the calculated values for time and position for total rod erosion correspond very well with the experimental data. So it can be stated that termination of failure front propagation—denoted by the dot-dash line—is delayed in time after total rod erosion occurs.

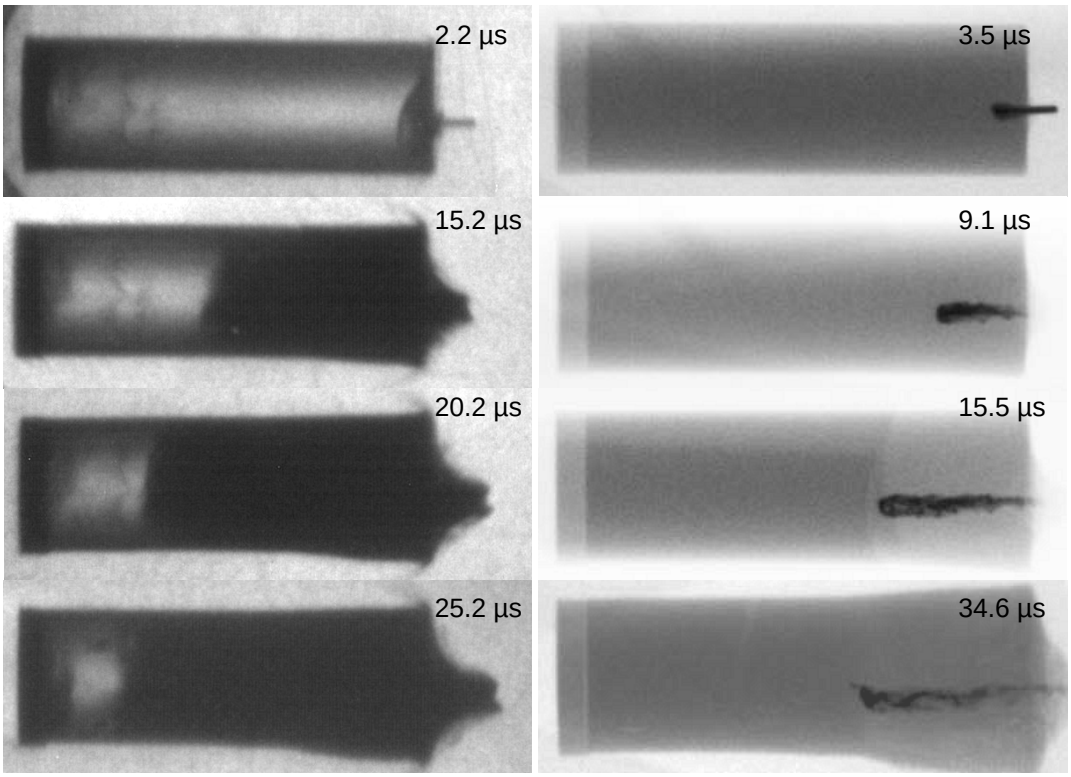

Figure 3. Camera pictures (left) and X-ray images (right) for Exp. 10864 (v_P = 2015 m/s); times after impact

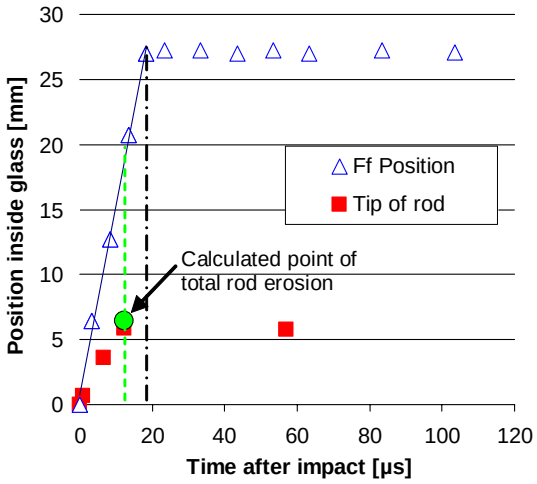

Figure 4. Failure front (Ff) and rod position inside glass after impact (Exp. 10848; v_P = 948 m/s)

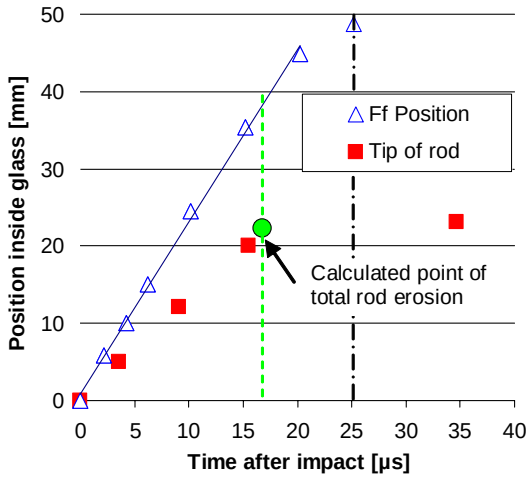

Figure 5. Failure front (Ff) and rod position inside glass after impact (Exp. 10864; v_P = 2015 m/s)

An interpretation of this observation is that when complete rod erosion occurs, there is no longer a stress at what was the rod/glass interface, and energy is no longer being transferred from the rod to the glass. This change in stress results in a rarefaction wave that propagates and overtakes the failure front, causing the failure front to stop. If this interpretation is correct, the data in Fig. 4 imply a speed of propagation of a rarefaction through the failed glass of about 3 km/s. This is about one-half the compressional wave speed in intact glass. The data in Fig. 5, although not definitive, are also consistent with a rarefaction wave speed of about 3 km/s in the failed glass.

Figure 6 shows u and v_C versus v_P while v_F versus v_P is illustrated in Fig 7. These figures also contain some data points for long-rod impact experiments that were done with 70-mm-long gold rods in a test set-up similar to the short-rod experiments [8]. It can be clearly seen that rod length does not influence the penetration and glass failure while there is an ongoing penetration process. Penetration of the rod itself shows a linear behaviour with increasing v_P. The slightly higher values of v_F for some of the short-rod experiments can be explained by the higher yaw angle on impact which can influence the determination of the exact point of impact and the position of the failure front inside the glass.

Target resistance R_T at the stagnation point of the penetration, Fig. 8, almost doubles in the considered impact velocity regime, indicating that the volume of comminuted material in front of the penetration is reduced with increasing v_P.

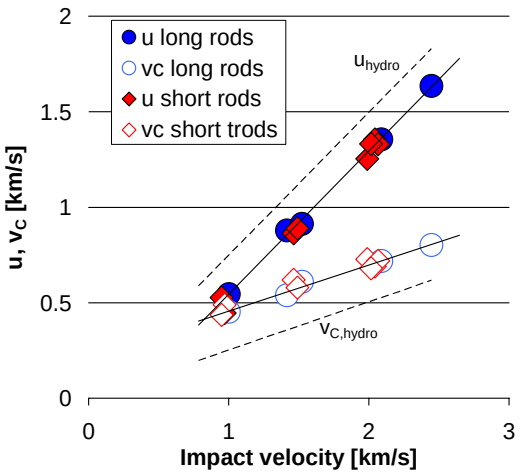

Figure 6. Penetration and consumption velocity versus impact velocity

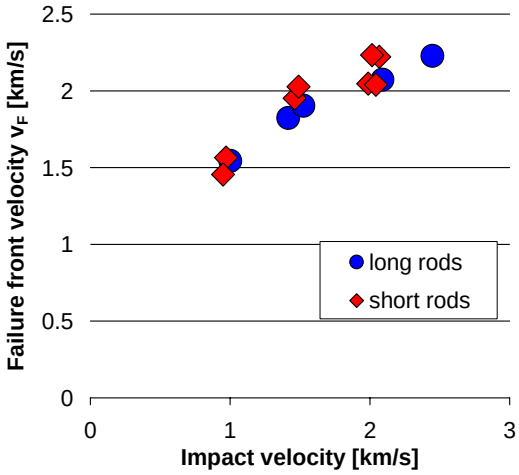

Figure 7. Failure front velocity versus impact velocity

Although the support of the gold rod is only a very thin strip of cello tape (or in the case of Exp. 10864, a thin polyamide filament), this support still has an influence on the glass target. In Figs. 2 and 3, the front face of the glass rod starts to disintegrate from side to side after impact with the supporting system. A test with only cello tape as the impactor confirmed this effect. However, failure inside the glass was of a magnitude less than with rod impact. Thus, it is considered that the influence of the rod support is negligible with respect to the effects from rod impact itself.

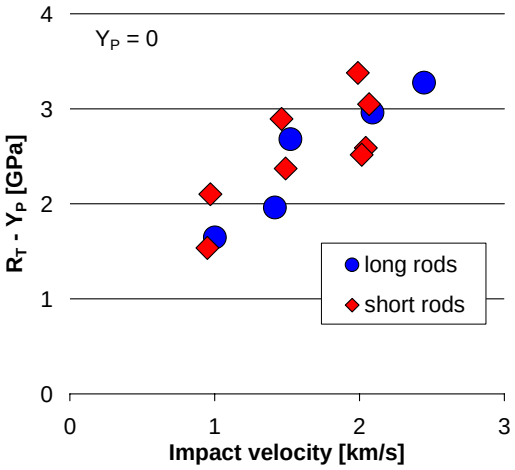

Figure 8. Target resistance R_T over impact velocity

SUMMARY AND CONCLUSIONS

Results for short-rod impact on borosilicate glass show that the failure front inside the glass arrests (comes to a standstill) after the rod is totally eroded. Once the rod is fully eroded, the driving stress for failure is removed. This supports an interpretation that failure of the glass is kinetics based; and that the term failure wave, which is often used in literature, is misleading. Interestingly, cessation of the propagating front is delayed in time from the point when the rod is completely eroded. A possible explanation for this effect implies a rarefaction wave speed in the failed glass of about 3 km/s. Failure front propagation in the glass before cessation, as well as penetration and consumption of the short rod, are steady-state processes. Penetration and consumption velocities show a linear increase with increasing impact velocity. The R_T value for target resistance doubles for the investigated velocities, increasing with the impact velocity. This suggests that for higher impact velocities, less damaged material is in front of the penetrator and target resistance tends toward the value of that for undamaged glass.

REFERENCES

1. S. J. Bless, and N. S. Brar, "Impact induced fracture of glass bars," *High-Pressure Science and Technology—1993* (Eds. S. C. Schmidt, J. W. Shaner, G. A. Samara, and M. Ross), pp. 1813-1816. New York: AIP Conference Proc. (1994).
2. H. D. Espinosa, Y. Xu, and N. S. Brar, "Micromechanics of failure waves in glass: I, Experiments," *J. Am. Ceram. Soc.* **80**, 2061-2073 (1997).
3. N. H. Murray, N. K. Bourne, J. E. Field, and Z. Rosenberg, "Symmetrical Taylor impact of glass bars", *Shock Compression of Condensed Matter—1997* (Eds. S. C. Schmidt, D. P. Dandekar, and J. W. Forbes) pp. 533-536. New York: AIP Conference Proc. (1998).
4. N. K. Bourne, J. C. F. Millett, Z. Rosenberg, and N. H. Murray, "On the shock induced failure of brittle solids," *J. Mech. Phys. Solids*, **46**, pp. 1887-1908 (1998).
5. Behner Th., Anderson Ch. E. Jr., Orphal D. L., Hohler V., Moll M., and Templeton D., "The failure kinetics of high density DEDF glass against rod impact at velocities from 0.4 to 2.5 km/s," *Proc. 22nd Int. Symp. Ballistics*, **2**, 877-884, DEStech Publications, Inc., Lancaster, PA (2005).
6. D. L. Orphal, Th. Behner, V. Hohler, C. E. Anderson, Jr., and D. Templeton, "Failure wave in DEDF and soda-lime glass during rod impact," *Shock Compression of Condensed Matter—2005* (M. D. Furnish, et al., Eds.), pp. 1391-1394, AIP Conf. Proc., Vol. 845 (2006).
7. P. Zeinert, S. J. Bless, and T. Beno, "Comminuted particles originating from catastrophic failure of a glass bar," *Shock Compression of Condensed Matter—2005*, (Eds. M. D. Furnish, et al.), AIP Conf. Proc, Vol. 845, pp. 900-902 (2006).
8. C. E. Anderson, Jr., T. Behner, D. L. Orphal, V. Hohler, and D. W. Templeton, "Failure kinetics of DEDF and borosilicate glass against rod impact," submitted for publication (2006).